

## Free-running, room temperature operation of an InGaAs/InP single-photon avalanche diode

Ryan E. Warburton,<sup>1,a)</sup> Mark Itzler,<sup>2</sup> and Gerald S. Buller<sup>1</sup>

<sup>1</sup>*School of Engineering and Physical Sciences, Heriot-Watt University, Edinburgh, EH14 4AS, United Kingdom*

<sup>2</sup>*Princeton Lightwave Inc., 2555 Route 130 South, Cranbury, New Jersey 08512, USA*

(Received 22 October 2008; accepted 20 January 2009; published online 20 February 2009)

Passive quenching operation of an InGaAs/InP single-photon avalanche diode detector at low excess bias is reported in terms of the key figures of merit including afterpulsing analysis. The reduced charge required to measure individual photon events meant that room temperature single-photon counting at 1550 nm wavelength was achievable without the requirement of electrical gating and with negligible afterpulsing effects evident. © 2009 American Institute of Physics.

[DOI: 10.1063/1.3079668]

Expanding application areas using single-photon detection have resulted in increased interest in single-photon detectors operating in the near infrared, including the InGaAs/InP single-photon avalanche diode (SPAD),<sup>1</sup> detectors based on SiGe,<sup>2</sup> and superconducting nanowire detectors.<sup>3</sup> InGaAs/InP SPAD detectors have been favored in a number of applications due to their high single-photon detection efficiencies (SPDE), low jitter, and operation at temperatures consistent with thermoelectric Peltier cooling. One of the major drawbacks of InGaAs/InP SPADs has been the severe operational limitations caused by the phenomenon of afterpulsing, although over the past few years several different electrical biasing schemes have been used to reduce its detrimental effects. For example, the use of a long blocking pulse after an event reduced the effects of afterpulsing at the expense of reduced count rates. Also, the use of short electrical gates of  $\sim 1$  ns duration permitted megahertz gating frequencies in Geiger mode InGaAs/InP avalanche photodiodes (APD) by several groups.<sup>4</sup>

Most approaches used to lessen the effects of the afterpulsing phenomenon involve an attempt to reduce the average charge per detection event. Gated quenching<sup>1</sup> is not ideal in all applications since the avalanche is not quenched until the gate is switched off, hence the average amount of charge per event will increase with gate duration. The use of a fast active quenching circuit (AQC) in conjunction with electrical gating makes a significant improvement to the effects of afterpulsing,<sup>5</sup> as the AQC can quench the avalanche rapidly after the event is detected. Use of an AQC enables a higher count rate to be achieved when compared to standard gating alone: at a hold-off time of 30  $\mu$ s the afterpulsing probability is reduced by two orders of magnitude. A similar method was reported by Liu *et al.* in Ref. 6.

Namekata *et al.*<sup>7</sup> used a sinusoidal gating scheme with an InGaAs/InP SPAD which increased the gating frequency to 800 MHz. By using a discriminator level two to three orders of magnitude lower compared to that typically used in square-wave gating, they were able to detect pulses of reduced charge flow through the device per avalanche event of  $\sim 10^5$  electrons (instead of  $10^7$ – $10^8$  under normal gating conditions). Namekata *et al.*<sup>7</sup> achieved 8.5% SPDE, with

only 6% afterpulsing probability with a dark count probability of  $9.2 \times 10^{-6}$  per gate. The maximum count rate achievable was estimated to be 6.5 Mcount/s when the average incident photon number was 0.1. Such results would not be possible in square-wave gating due to the capacitive response of the SPAD, which would produce transients of greater amplitude than the avalanche signal itself. Yuan *et al.*,<sup>8</sup> developed a technique where the SPAD output is split with one signal delayed by a clock cycle and one output being subtracted from the other by means of a differencing circuit, resulting in weak avalanche pulses being detected that would otherwise be hidden in the transient response of the capacitive circuit. With this approach, the detector could be used at 1.25 GHz, with an SPDE of 10.8%, an afterpulsing probability of 6.16%, and a count rate that saturated at 100 Mcount/s. Other approaches, such as that demonstrated by Zhao *et al.*,<sup>9</sup> detailed the use of an internal energy barrier within an InGaAs/InAlAs SPAD to create a self-quenching mechanism for operation at a wavelength of 1550 nm. This device showed good SPDE at an operating temperature of 160–240 K, but recovery times of 10s ns were long compared to that described below.

The methods of sinusoidal gating and self-differencing permit high gating frequencies and a significant reduction in the afterpulsing phenomenon. Since the gates are periodic and of subnanosecond duration in both cases, these methods are more suited for use in a QKD system where the precise timing window of potential photon (or bit) arrivals can be predicted. However, such a gating approach is not ideal for applications like time resolved photoluminescence (TRPL),<sup>10</sup> where lifetimes may range from subnanosecond to many tens of nanoseconds, and photon-counting time-of-flight ranging<sup>11</sup> if distances to targets are unknown. We describe a quenching approach that utilizes a very low average level of charge per event in order to reduce afterpulsing in InGaAs/InP SPADs, which can permit fully free-running operation.

For the following measurements, a 25  $\mu$ m diameter Princeton Lightwave InGaAs/InP SPAD was used. The SPAD was reverse biased by a constant dc voltage through a series resistor  $R_S$  (values of 10 k $\Omega$ , 100 k $\Omega$ , and 1 M $\Omega$  were chosen for  $R_S$ ) and the output was measured across a 50  $\Omega$  resistance, usually by an oscilloscope or the input of a photon counting card. While this quenching mode is a form

<sup>a)</sup>Electronic mail: r.e.warburton@hw.ac.uk.

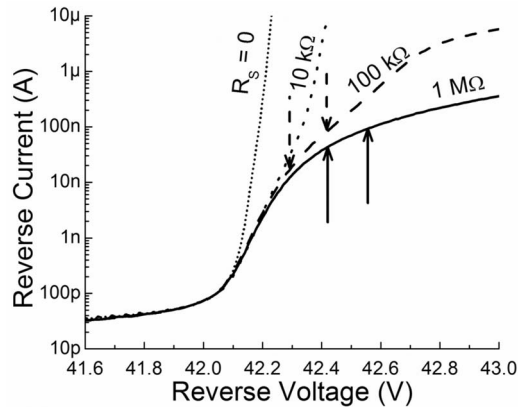


FIG. 1. Reverse  $I$ - $V$  characteristic of an InGaAs/InP SPAD at 270 K using different values of  $R_S$ , all performed under dark conditions. The dashed black arrows indicate the minimum and maximum voltages used when  $R_S = 100$  k $\Omega$  and the solid arrows for  $R_S = 1$  M $\Omega$ .  $R_S = 0$  and 10 k $\Omega$  are shown for comparison.

of passive quenching, as described in detail in Ref. 12, in these experiments the device is operated at a low excess bias, permitting a low peak current flow. Such a biasing approach can only be attempted with a low dark current device and the rapidity of the quenching process will depend on the product of the diode series resistance (in conducting mode) with the sum of the device capacitance and stray capacitance. In this case the diode series resistance is  $< 2$  k $\Omega$  and the overall device capacitance is less than 0.5 pF. At the low excess bias levels used in this quenching approach, the overall SPAD output pulse is a few nanosecond duration and 5 mV in amplitude meaning that the overall charge per event is greatly reduced to  $\sim 1 \times 10^6$ , which is low compared with more typical passive quenching or gated quenching approaches described previously,<sup>1</sup> and results in a significant lessening of the effects of the afterpulsing phenomenon, as shown below. It is this low excess bias passive quenching and combination of critical device characteristics that has permitted room temperature operation of the InGaAs/InP SPAD in an entirely free-running mode without any requirement for electrical gating.

Using similar photon-counting characterization techniques to those described in detail by us in Ref. 1, the SPDE, dark count rate (DCR), and noise-equivalent power (NEP) of the SPAD could be measured using 1550 nm wavelength illumination. A low noise amplifier (LNA1000 by RF Bay Inc.) was employed to increase the pulse height for compatibility with commercial photon counting data acquisition modules. In these measurements, we used a data acquisition card with a constant fraction discriminator (CFD) input. The CFD level was constant throughout the measurements described below. The measurements were recorded at each discrete bias voltage and over a range of temperatures from 170 to 290 K.

Figure 1 shows the reverse  $I$ - $V$  characteristic for an InGaAs/InP SPAD at 270 K in the vicinity of avalanche breakdown using the three different values of  $R_S$  and no  $R_S$ . The effect of using a higher resistance for  $R_S$  on the operating voltage is shown in Fig. 1. For example, with the 100 k $\Omega$  resistor, the operating voltages lie between the two dashed arrows. At reverse biases above this range, SPDE measurements could not be made due to the prohibitively high DCR. For a given  $R_S$ , use of a higher overall bias results

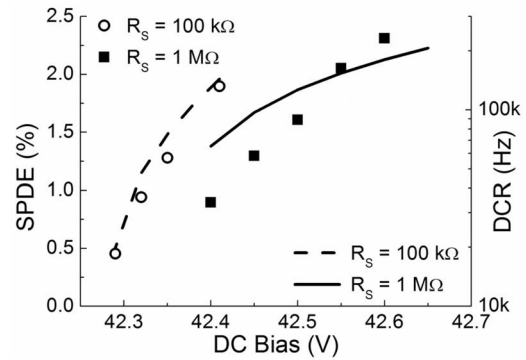


FIG. 2. SPDE at  $\lambda \sim 1550$  nm (plotted as symbols, left-hand y-axis) and DCR (plotted as lines, right-hand y-axis) vs reverse dc bias of an InGaAs/InP SPAD operated in low excess bias passive quenching at 270 K with  $R_S$  of 100 k $\Omega$  and 1 M $\Omega$ .

in a larger electric field within the device and hence a greater SPDE, as shown in Fig. 2.

Figure 2 shows the differences observed in SPDE and DCR with bias at two different values of  $R_S$ . When  $R_S$  was increased to 1 M $\Omega$ , although the SPDE at equivalent overall voltage was lower since the voltage across the diode was reduced by the drop across the larger  $R_S$ , the capability of increasing the bias could be realized due to the reduced gradient of the dark current with increasing bias level. Throughout the temperature range measured, the maximum SPDE when  $R_S = 100$  k $\Omega$  was  $\sim 2.5\%$  and up to 3% for  $R_S = 1$  M $\Omega$ . Similarly, when operated at the same overall bias, an increase in  $R_S$  corresponded to a lowering of DCR since proportionally more of the bias was dropped across the resistor rather than the diode when the avalanche was flowing. As expected with the increased electric field, the highest SPDE condition found with  $R_S = 1$  M $\Omega$  corresponded to the a minimum in timing jitter of  $\sim 500$  ps full width at half maximum (FWHM).

The SPDE values are generally lower than in gated Geiger mode measurements, however, the DCRs are also much reduced. A comparison of the NEP between Geiger mode (using gated quenching) and low excess bias passive quenching is shown in Fig. 3. In each case, the minimum NEP is shown for each operating temperature, although this does not necessarily represent the point of highest SPDE or lowest DCR. Using the same threshold level, the 100 k $\Omega$  and 1 M $\Omega$  series resistance give very similar NEP values. The

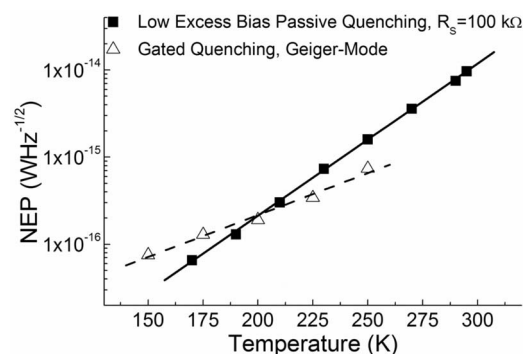


FIG. 3. NEP at  $\lambda \sim 1550$  nm vs temperature for gated Geiger mode operation (empty symbols, dotted line) and low excess bias passive quenching when  $R_S$  was 100 k $\Omega$ . The Geiger mode measurements were performed with a gate duration of 50 ns.

gated Geiger-mode measurements were not performed at temperatures above 250 K due to the increased DCR.

We also examined how the gain of the SPAD in this quenching mode changed with voltage to examine the tolerance to bias fluctuations. Assuming an  $R_S$  of 100 k $\Omega$  in the bias range of operation, a 100 mV variation in bias results in a change to the total charge measured per event of  $\sim 30\%$ . In the measurements described in this paper it was possible to control the dc bias in 10 mV steps. This accuracy is sufficient to keep the charge flow steady to within  $\sim 3\%$ . In terms of temperature variation, the breakdown voltage changes by 0.17 V/K.<sup>1</sup> In these experiments, the temperature stability was better than 0.1 K, therefore the breakdown voltage varied by a maximum of  $\sim 20$  mV, resulting in a maximum change in gain of  $\sim 6\%$ . In practice, however, the use of thresholding circuitry and, in particular, CFD, meant that bias and temperature instabilities of such a magnitude will have negligible effect on measured device performance.

From the results presented thus far, there are several advantages of using a high value of  $R_S$ : higher SPDE and lower jitter. However, the penalty is the limitation in the maximum count rate that the detector is capable of achieving due to the recharging effect of the diode through the larger resistor. To investigate this effect, the photon flux was increased and the count rate measured until a saturation point was reached and the count rate was maximized. When  $R_S=100$  k $\Omega$  the maximum count rate is  $\sim 4$  Mcount/s, however, with  $R_S=1$  M $\Omega$  the count rate saturates at  $\sim 400$  kcount/s.

As the count rate increases, the average current passing through the SPAD necessarily increases. Although the number of charge carriers per event is significantly lower than in gated Geiger mode, the effects of afterpulsing remain evident, especially at low temperatures. In this low excess bias passive quenching mode, afterpulsing is manifested as an increase in the dark background level (and correspondingly reduced peak to background ratio) in a timing histogram measurement of a repetitive pulsed optical input. We can examine this using photon count histograms for varying incident optical signals, as shown in Fig. 4, which shows a series of histograms at both 290 and 250 K. As can be seen in Fig. 4, at the higher temperature of 290 K, there is little effect on the background with increasing photocount rate up to  $10^6$  counts per second indicating negligible effects of afterpulsing. By comparison, the results at 250 K shown in the inset of Fig. 4 show a significant increase in background with varying photon flux, as the effect of afterpulsing is significant at this temperature.

In summary, we characterized a Princeton Lightwave Inc. InGaAs/InP SPAD in low excess bias passive quenching mode at temperatures between 170 and 290 K. Due to the thresholding of the dark counts, the device performance relied on a careful selection of series resistance, in this case a minimum NEP was found using  $R_S=100$  k $\Omega$ . The use of a larger  $R_S$  meant a reduction in dark count rate, enabling a higher voltage to be used which resulted in a both a higher

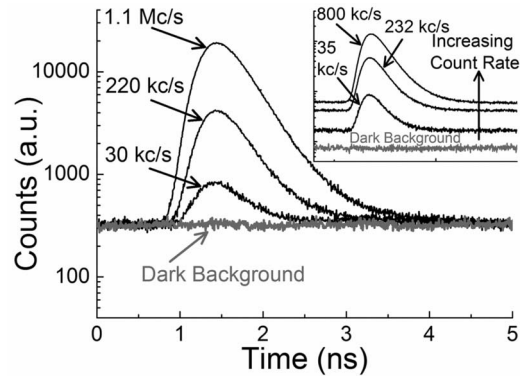


FIG. 4. Timing histograms at different incident photon fluxes for the SPAD in low excess bias passive quenching operation using an  $R_S$  of 100 k $\Omega$  at a temperature of 290 K. The inset shows a comparison of similar photon counting traces at 250 K. The scales on both sets of axes are identical and the dark background is shown in gray.

maximum SPDE and reduced jitter ( $\sim 500$  ps FWHM). The penalty of using a larger  $R_S$  results in a lower maximum count rate as the reset time depended on the  $R_S C$  time constant of the circuit. With an  $R_S$  of 100 k $\Omega$ , a maximum count rate of 4.0 Mcount/s, whereas only 400 kcount/s was reached with an  $R_S$  of 1 M $\Omega$ . Finally the afterpulsing effects were studied in this quenching mode by increasing the photon flux arriving at the SPAD. The DCR was observed to be progressively less dependent on photon flux with increasing temperature. Finally, at 290 K it was shown that an InGaAs/InP SPAD could be operated with no electrical gating and with negligible afterpulsing effects evident.

The authors acknowledge support from the Framework Six SECOQC Project (ref.506313).

- <sup>1</sup>S. Pellegrini, R. E. Warburton, L. J. J. Tan, J. S. Ng, A. B. Krysa, K. Groom, J. P. R. David, S. Cova, M. J. Robertson, and G. S. Buller, *IEEE J. Quantum Electron.* **42**, 397 (2006).
- <sup>2</sup>A. Y. Loudon, P. A. Hiskett, G. S. Buller, R. T. Carline, D. C. Herbert, W. Y. Leong, and J. G. Rarity, *Opt. Lett.* **27**, 219 (2002).
- <sup>3</sup>G. N. Gol'tsman, O. Okunev, G. Chulkova, A. Lipatov, A. Semenov, K. Smirnov, B. Voronov, and A. Dzardarov, *Appl. Phys. Lett.* **79**, 705 (2001).
- <sup>4</sup>P. L. Voss, K. G. Köprülü, S.-K. Choi, S. Dugan, and P. Kumar, *J. Mod. Opt.* **51**, 1369 (2004).
- <sup>5</sup>S. Cova, A. Tosi, A. Gulinatti, F. Zappa and M. Ghioni, *IEEE LEOS Newsletter* **20**, 25 (2006).
- <sup>6</sup>M. Liu, C. Hu, J. C. Campbell, Z. Pan, and M. M. Tashima, *IEEE J. Quantum Electron.* **44**, 430 (2008).
- <sup>7</sup>N. Namekata, S. Sasamori, and S. Inoue, *Opt. Express* **14**, 10043 (2006).
- <sup>8</sup>Z. L. Yuan, B. E. Kardynal, A. W. Sharpe, and A. J. Shields, *Appl. Phys. Lett.* **91**, 041114 (2007).
- <sup>9</sup>K. Zhao, S. You, J. Cheng, and Y. Lo, *Appl. Phys. Lett.* **93**, 153504 (2008).
- <sup>10</sup>G. S. Buller, S. J. Fancey, J. S. Massa, A. C. Walker, S. Cova, and A. Lacaita, *Appl. Opt.* **35**, 916 (1996).
- <sup>11</sup>G. S. Buller and A. M. Wallace, *IEEE J. Sel. Top. Quantum Electron.* **13**, 1006 (2007).
- <sup>12</sup>S. Cova, M. Ghioni, A. Lacaita, C. Samori, and F. Zappa, *Appl. Opt.* **35**, 1956 (1996).